보건학석사 학위논문

Degradation Kinetics and Mechanism of Cyclophosphamide during UV/chlorine process.

UV/chlorine 공정 중 Cyclophosphamide의

분해 특성과 메커니즘에 관한 연구

2019년 2월

서울대학교 보건대학원

환경보건학과 환경보건학전공

이 지 영

Abstract

Degradation Kinetics and Mechanism of Cyclophosphamide during UV/chlorine process.

Ji-Young Lee
Department of Environmental Health
Graduate School of Public Health
Seoul National University

Cyclophosphamide, which is widely used as an anticancer drug, has severe health effects such as non-target organ damage. According to monitoring studies, cyclophosphamide was widely detected in hospital wastewater and in surface water. Since cyclophosphamide is not only non-biodegradable, but it also rarely removed in conventional treatments in wastewater treatment plant (WWTP). Therefore, the alternative treatment process is needed. In this study, the removal of cyclophosphamide using UV/chlorine process using UV-B lamp was examined. Cyclophosphamide was not degraded by UV photolysis and dark chlorination

treatment. However, combined UV/chlorine process was effective for cyclophosphamide degradation (k_{obs} = 1.98 × 10^{-1} min^{-1} (R^2 = 0.93)). The higher rate constants were observed when the free available chlorine (FAC) concentration was high and acidic pH. More than 56% of cyclophosphamide was mineralized within 8 hours during the reaction. Seven organic byproducts (m/z = 141.01, 192.10, 198.03, 212.01, 258.01, 274.00, 276.02), and five inorganic byproducts (NH_3, NO_3^-, $HCOO^-$, PO_4^{3-}, and ClO_3^-) were identified using LC-qTOF-MS and ion chromatography. Toxicity test using *V. fisheri*, showed that inhibition of luminescence of the *V. fisheri* increased to 88% as the reaction proceeded during the UV/chlorine process. Our results imply that UV/chlorine process can be applied to cyclophosphamide contaminated water and wastewater.

Keywords: Cyclophosphamide, Anticancer, UV-B/chlorine process, Byproducts, Acute toxicity

Student Number: 2017-24362

List of Tables

List of Figures

Contents

1. Introduction

1.1. Backgrounds

There is a rising problem of water pollution caused by chemical substances in accordance with the increase of global chemical consumption and production (Margot, Rossi, Barry, & Holliger, 2015). Especially, the release of micro-pollutants that have not been completely removed from wastewater treatment plants (WWTP) into surface water can have adverse effect of both direct or indirect to the human health through drinking water as well as ecosystem (Luo et al., 2014; Schwarzenbach et al., 2010).

Anticancer drugs, one of the classes of cytotoxic drugs (CSDs), can inhibit cell growth, directly kill cells, show potential carcinogenicity, genotoxicity, and affect both targeted and non-targeted cell in low concentrations (Zhang, Xiao, Zhang, Chang, & Lim, 2017). Among CSDs, cyclophosphamide (CP) is widely used as an anticancer drug, and its annual consumption is 200-400 kg/yr at Germany (Buerge, Buser, Poiger, & Müller, 2006). CP is effective in the treatment of Hodgkin's lymphoma, chronic myeloid leukemia, breast cancer and uterine cancer. However, CP is classified as a group 1 of the carcinogens designated by the International Agency for Research on Cancer (IARC, 2016). CP also has side effect such as

bladder bleeding, lymphomas, and decreasing number of red blood cells, white blood cells and platelets (Jalali, Hasanzadeh, & Malekinejad, 2012), so it requires caution.

In addition, since CP is not biodegradable (Buerge et al., 2006; TKKHA Steger-Hartmann, Kümmerer, & Hartmann, 1997; Thomas Steger-Hartmann, Kümmerer, & Schecker, 1996), and rarely adsorbed to sludge or sediment due to low log K_{ow} value (log K_{ow} = 0.63), typical biologic and physical treatment in WWTP cannot remove the CP efficiently (Buerge et al., 2006; Ternes et al., 2005). CP also can exist in hospital wastewater through urine and feces of patients who undergoes chemotherapy. According to monitoring studies (Table 1), CP was detected in hospital wastewater the concentrations of up to 2,000 ng/L in China and 22,000 ng/L in Slovenia respectively (Česen et al., 2015; Yin, Shao, Zhang, & Li, 2010). It was also detected in WWTP effluent the concentrations of average 13.1 ng/L and 100 ng/L in Spain and France, respectively (Catastini et al., 2008; Gómez-Canela et al., 2012). Moreover, it was also detected in surface water, the concentrations of maximum 100 ng/L and 64.8 ng/L at Australia and Rumania, respectively (Busetti, Linge, & Heitz, 2009; Moldovan, 2006). Thus, effective removal of CP using alternative treatment is needed. Recently, the studies that removing CP by advanced oxidation process (AOP) have been conducted.

Table 1. Concentration of cyclophosphamide at wastewater, and surface water.

	Country	Conc. (ng/L)	Ref.
Hospital WWTP effluent	China	6−2000	Yin et al. (2010)
	Slovenia	14−22000	Česen et al. (2015)
WWTP influent	Spain	<LOD-13100	Gómez-Canela et al. (2012)
	Slovenia	<34	Isidori et al. (2016)
	Spain	<LOQ-43.8	Negreira, de Alda, and Barceló (2014)
WWTP effluent	Spain	<LOQ-25.0	Negreira et al. (2014)
	Australia	<125	Busetti et al. (2009)
	France	300	Catastini et al. (2008)
Surface water	Australia	<100	Busetti et al. (2009)
	Romania	0-64.8	Moldovan (2006)

1.2. Advanced oxidation processes (AOPs) studies on degradation of cyclophosphamide

Advanced oxidation processes (AOPs) is hydroxyl (OH) radical formation processes including ozone, UV related AOP, photocatalyst, and electrochemical oxidation. The goals of AOPs are enhanced degradation, detoxification, and biodegradability using free radicals, such as OH radicals and other reactive halogenated species. Those radicals are working as powerful oxidants that can break non-biodegradable organic chemicals (Glaze, Kang, & Chapin, 1987; Glaze & Kang, 1989).

Table 2 shows AOP studies which remove cyclophosphamide (CP) such as using UV/H_2O_2, and UV/TiO_2. Lutterbeck et al (Lutterbeck, Machado, & Kümmerer, 2015) removed CP using UV/H_2O_2, UV/Fe^{2+}/ H_2O_2, and UV/TiO_2 processes, the removal rate was fastest when using UV/Fe^{2+}/ H_2O_2, and rate constant was 1.35×10^{-1} min^{-1}. They identified byproducts by LC-MS/MS and did the acute and chronic toxicity test using *V. fisheri*. UV/ H_2O_2 process was applied in the study of Zhang et al (Zhang et al., 2017). They found that as the concentration of H_2O_2 increased, the reaction rate was faster. However, reaction rate decreased from a certain amount due to scavenging effect of OH radical. It was also observed that the reaction rate was slower as the pH increased. Lai et al (Lai, Chuang, & Lin, 2017) studied removal trend of CP that presence of anions such as HCO_3^-, Cl^-, NO_3^-, and SO_4^{2-} during

UV/TiO_2. As the concentration of anions increased, the removal rate was decreased generally. Also, the toxicity test using *V. fisheri* showed that, the toxicity was increased when concentration of anions increased. Furthermore, VIS-photocatalyst process using Pt-TiO_2 under sunlight was studied by Ofiarska et al (Ofiarska, Pieczyńska, Borzyszkowska, Stepnowski, & Siedlecka, 2016). They showed that CP was not degraded by only sunlight photolysis, and the removal rate was faster when Pt was combined with TiO_2 process than only TiO_2 process. Also, the time profile, structure, and pathway of the byproducts were identified at both TiO_2 and Pt-TiO_2 processes by using LC-MS/MS.

Table 2. Preliminary studies about advanced oxidation process for cyclophosphamide.

Process	Kinetics	Byproduct	Toxicity	Reference
UV/H_2O_2, UV/Fe^{2+}/H_2O_2, and UV/TiO_2	O	O	O	Lutterbeck et al. (2015)
TiO_2	O	O	O	Lai, Lin, and Lin (2015)
UV/TiO_2	O	O	O	Lai et al. (2017)
Sunlight-Pt-TiO_2	O	O	X	Ofiarska et al. (2016)
UV/H_2O_2	O	O	X	Zhang et al. (2017)
UV photolysis, UV/H_2O_2, and Sunlight	O	X	X	Franquet-Griell, Medina, Sans, and Lacorte (2017)
TiO_2	O	X	X	Constantin, Cristea, Nitoi, Constantin, and Nechifor (2017)
Ozonation	O	X	X	Garcia-Ac et al. (2010)
UV photolysis, ozonation, and UV/O_3	O	X	X	Česen et al. (2015)
O_3/H_2O_2	O	X	X	Fernández et al. (2010)

1.3 Objectives

Through the preliminary studies, it was proved that removing cyclophosphamide (CP) by UV-AOP was effective. However, additional substances such as TiO_2 or H_2O_2.are needed. It is disadvantageous in economic terms compared to UV/chlorine process because TiO_2 or H_2O_2 were more expensive than chlorine. The advantage of UV/chlorine process is easily applicable to WWTP systems since chlorination is currently already used as disinfection purpose in the WWTPs, only UV lamps are needed for the application of UV/chlorine process. Also, UV/chlorine process has additional disinfection function due to residual chlorine.

Therefore, the objectives of this study are (1) to observe the removal kinetics of CP through UV/chlorine process, (2) to examine the removal rate when response factors were changed, (3) to identify the byproducts during the process, and (4) to investigate the toxicity during the process.

2. Material and method

2.1. Chemicals

Cyclophosphamide monohydrate (analytical standard) was purchased from Sigma-Aldrich (St. Louis, MO USA). Sodium hypochlorite (NaOCl), sodium thiosulfate ($Na_2S_2O_3$), formic acid (CH_2O_2), sodium carbonate (Na_2CO_3), sodium bicarbonate ($NaHCO_3$), and sodium formate (NaHCOO) were purchased from (St. Louis, MO USA). Methanol (Optima, Fisher scientific UK Limited) was used as mobile phase when using UHPLC-MS/MS and UPLC-qTOF-MS.

Table 3. Physcico-chemical properties of cyclophosphamide.

Structure	Properties	
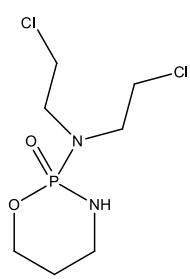	Chemical formula	$C_7H_{15}Cl_2N_2O_2P$
	Molecular weight	261.086
	pKa	2.84
	Solubility in water	5943mg/L at 25℃

2.2. Experimental procedure

2.1.1. Kinetics

To examine the removal kinetics of cyclophosphamide (CP), UV-photolysis, chlorination, UV/chlorine process reactions were conducted using a batch type photoreactor equipped with UV-B mercury lamp (312 nm, 6 W, San-Kyo Electrics, Japan) (Figure 1). The intensity of UV-B lamp was 1.8 ~ 2.2 mW/cm^2 which was measured by a radiometer (VLX-3W Radiometer 9811-50, Cole-Parmer, USA).

Powdered CP was dissolved in deionized water from Milli-Q Water Purification System (Millipore, Burlington, MA, USA). And the stock solution was made just before the experiment. Initial concentration of CP was 0.1 mg/L for the removal kinetics, 1 mg/L for the organic byproduct identification, and 10 mg/L for mineralization and inorganic byproduct identification.

For UV/chlorine experiments, NaOCl was first added in a batch type photoreactor containing 2 L of deionized water, then solution was mixed with magnetic bar and magnetic stirrer. Next, the pH was adjusted using 1 M sulfuric acid (H_2SO_4) and 1 M sodium hydroxide (NaOH), the stock solution of CP was added, and last, UV lamp was inserted. UV photolysis or chlorination experiment is like UV/chlorine experiment without NaOCl solution or UV lamp.

The initial concentration of CP in the experiments for the removal kinetics was 0.1 mg / L, for identification of organic byproducts and environmental toxicity tests was 1 mg / L, for mineralization and identification of inorganic byproducts is 10 mg / L. The reason for the different initial concentration of CP in each experimental procedure was that the concentration ranges for obtaining stable and suitable results in each instrument was different. The initial concentration of free chlorine (Cl_2) was 0.4, 2, 6, 10, and 14 mg/L for kinetics of chlorine effect, 10 mg/L for identification of organic byproducts and acute toxicity test, and 140 mg/L for mineralization and identification of inorganic byproducts. After sampling, the sodium thiosulfate ($Na_2S_2O_3$) solution was injected 1.5 times to the residual chlorine concentration to use as a chlorine quencher to terminate the response.

2.1.2. Toxicity test

Acute toxicity test was conducted by Microtox Model 500 Toxicity Analyzer. The intensity of luminescence was measured using bioluminescent bacteria, *Vibrio Fisheri*. The experiment was following the protocol of 81.9% basic test, and the pH of the treated samples were adjusted between 6 and 8 with 0.1M H_2SO_4 and 0.1M NaOH, at which the bacteria were activated. The toxicity of each byproduct were evaluated by QSAR software (OECD Tool Box V.4.2).

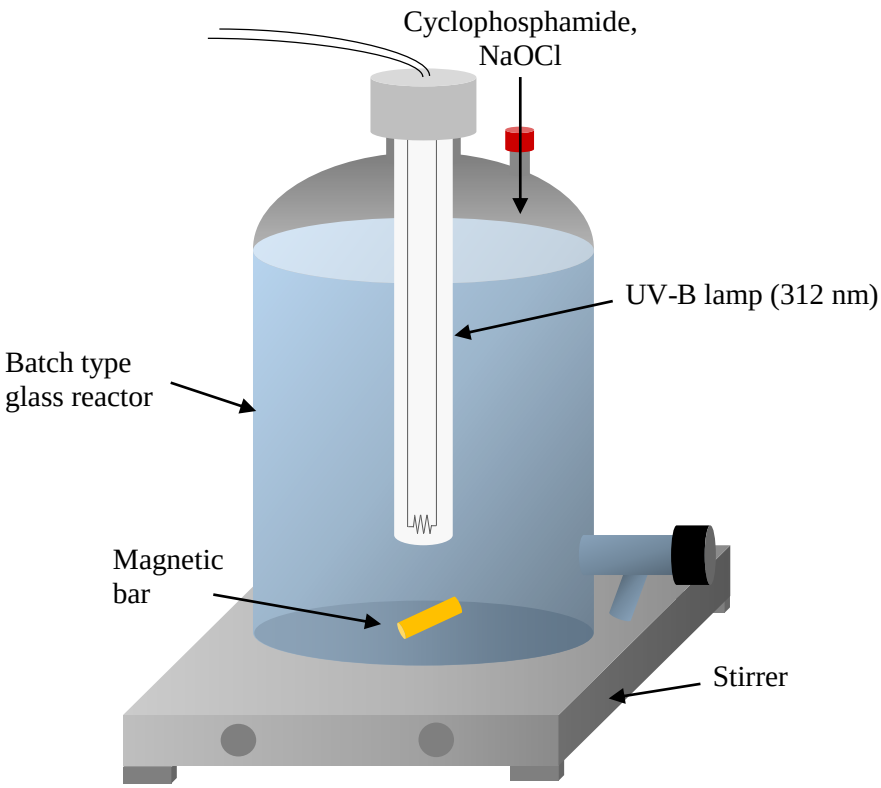

Figure 1. The schematic diagram of the batch type reactor system.

2.3. Analytical method

2.3.1. Analysis with UHPLC-MS/MS

UHPLC (Nexera, Shimadzu, Japan) equipped with tandem mass spectrometer (API 4000, AB Sciex, CA, USA) was used for analyzing the removal kinetics of cyclophosphamide (CP). The mobile phases were 0.1% formic acid in water (A) and 0.1% formic acid in MeOH (B), and they were performed in isocratic mode with mobile phase B 75%. The total analysis time was 8 min, at a flow rate 0.3mL/min. Luna® Phenyl-Hexyl column (100 mm × 4.6 mm, 3 μm, Phenomenex, Torrance, CA, USA) was used, and the column oven temperature was 40℃. Electrospray ionization (ESI) was used in positive mode, and multi reaction monitoring (MRM) mode was used to detect CP. The MRM method of CP is in Table 4. Data processing was performed by Analyst® software 1.6.1 (AB Sciex, CA, USA).

Table 4. The MRM method of cyclophosphamide for UHPLC-MS/MS

Precursor ion (m/z) (Da)	Product ion (m/z) (Da)	DP (V)	CE (V)	CXP (V)
262.655	142.000	46	33	10
	120.000	46	31	12
	106.300	46	29	22

* DP: Declustering potential, CE: Collision energy, CXP: Collision cell exit potential

2.3.2. Analysis of byproducts

ACQUITY UPLC equipped with Synapt G2-S triple quadrupole mass spectrometer (Waters, Milford, MA, USA) was used for screening and identification of organic byproducts of cyclophosphamide during UV/chlorine process. Analysis methods were divided into two as shown in Table 5. Method 1 was same as the method of detecting Cyclophosphamide in LC-MS/MS in 2.3.1. Method 2 referred to (Lai et al., 2017), reducing the flow rate to 0.5 ml/min and increasing the analysis time to 14 min.

Table 5. LC-qTOF-MS conditions for byproducts analysis.

	Method 1	**Method 2**
Column	Luna® Phenyl-Hexyl column (100 mm × 4.6 mm, 3 μm)	Kinetex C18 column (100 mm × 2.1 mm, 1.7 μm)
Mobile phase	(A) 0.1% formic acid in water (B) 0.1% formic acid in MeOH	(A) 5mM ammonium acetate in water (B) 5mM ammonium acetate in MeOH
ESI mode	Positive and negative	Negative
Mobile phase composition	Isocratic mode (B) = 75%	Gradient mode (B) = 0% (0 min) → 95% (4 min) → 98% (19 min) → 0% (10 min) → 0% (14 min)

The samples of UV/chlorine process were analyzed by UNIFI software (Waters, Milford, MA, USA) to screening and identifying byproducts in MSe continuum mode, and analyzed once again by Masslynx software (Waters, Milford, MA, USA) to identifying byproducts in MSe centroid mode. The high resolution mass spectrometry (HRMS) methods of the instrument are on Table 6.

Table 6. High resolution mass spectrometry (HRMS) conditions for LC-qTOF-MS analysis

Mass parameters	Value
Caplilary voltage	2.8 kV
Sampling cone voltage	30 V
Source offset	80
Source temperature	100 ℃
Desolvation temperature	250 ℃
Desolvation gas flow	800 L/hr

The method for identifying the byproducts were as follows; First, using UNIFI software, unknown unique compounds that do not overlap with untreated sample were sorted out, and candidates that has a time profile and mass tolerance of less than 5 ppm were sorted out too. Next, got the chemical formula of the candidates from Masslynx software was obtained, and drew the chemical structure with

Chemdraw Ultra 12.0 (CambridgeSoft, Waltham, MA, USA). Finally, the chemical structure was added to UNIFI software to match the chemical on the chromatogram and identifying the byproducts.

TOC analyzer (TOC 5000, Shimadzu, Kyoto, Japan) was used for confirming the TOC concentration and mineralization rate of the UV/chlorine process treated samples. Ion chromatography (IC) Dionex ICS-1100 (Thermo Fisher Scientific, USA) was used for analyzing the concentration of chlorate (ClO_3^-), formate ($CHOO^-$), and nitrate (NO_3^-) ions. To separate the ions, IonPac AG 14 guard column (50 mm x 4 mm) and IonPac AS14 column (250mm x 4mm) were used, and Dionex AERS 400 was used as a electrolytically regenerated suppressor. To measure the chlorite, chlorate, and formate ion, a mixed solution of 2.7mM Na_2CO_3 and 1.0mM $NaHCO_3$ was used as an eluent. Also, mixed solution of 3.5mM Na_2CO_3 and 1.0mM $NaHCO_3$ was used for measure the nitrate ion as an eluent. Humas water analyzer was used to identify the inorganic byproducts that concentration of under limit of detection of IC. The treated samples and color developing reagents were added to the water test kits for color development, and the concentration of the inorganic byproducts, ammonia (NH_3), and phosphate (PO_4^{3-}) were measured with a Humas water analyzer (HS-2300 Plus, Humas, Korea).

2.3.3. Analysis of experimental condition

For scanning the absorbance cyclophosphamide (CP) in UV wavelength range, Infinite M200 (TECAN, Mannedorf, Swiss) was used. CP was analyzed at the concentrations of 0.1 mg/L at pH 4, 7, and 10. To measure the residual chlorine concentration during UV/chlorine process, measure with the HACH DR-890 colorimeter (HACH, Loveland, CO, USA) using the N, N-diethyl-p-phenylenediamine color regent. The NeoMet pH/ORP meter pH-220L (iSTEK, Korea) was used for measuring the initial pH before the processing. To adjust the pH, 1M sulfuric acid (H_2SO_4) and 1M sodium hydroxide (NaOH) was used.

3. Results and Discussion

3.1. Degradation kinetics of cyclophosphamide during UV-photolysis, chlorination, and UV/chlorine process.

The results of the degradation of cyclophosphamide (CP) with UV-photolysis, dark chlorination, and UV/chlorine process over time is on Figure 2. Compared to UV-photolysis and dark chlorination, UV/chlorine process effectively removed CP. The reason why CP was not removed from UV-photolysis and dark chlorination is due to stable structure of CP, with an alkyl chain with two chlorine atoms. Franquent-Griell (Franquet-Griell et al., 2017) also found that CP was not removed form UV-C light (254 nm). The UV/chlorine process followed pseudo-first order kinetics with observed rate constants (k_{obs}) of 1.98×10^{-1} min^{-1} ($R^2 = 0.93$) (Franquet-Griell et al., 2017).

In the UV/chlorine process, free chlorine species are available in three forms in water depending on pH (Cl_2, HOCl and OCl^-). Especially HOCl and OCl^- are producing OH radicals and reactive chlorine species when it subjected to UV radiation (Eq. (2) - (4)). Generally, CP is removed by UV photon, OH radical and reactive chlorine species. Therefore, more radicals were produced when the two

processes were combined, resulting in higher removal efficiency than the single process. The mechanism of radical formations (Fang, Fu, & Shang, 2014) and removing CP in UV/chlorine process are suggested below.

$$HOCl \rightleftharpoons H^+ + OCl^- \quad (pKa = 7.6) \tag{1}$$

$$HOCl \xrightarrow{UV} \bullet OH + \bullet Cl \quad (pH < 7.6 \text{ at } 25℃) \tag{2}$$

$$OCl^- \xrightarrow{UV} \bullet O^- + \bullet Cl \quad (pH > 7.6 \text{ at } 25℃) \tag{3}$$

$$\bullet O^- + H_2O \rightarrow \bullet OH + OH^- \tag{4}$$

$$CP + UV \text{ photon} \rightarrow \text{Byproducts (direct)} \tag{5}$$

$$CP + \bullet OH \text{ or } \bullet Cl \rightarrow \text{Byproducts (indirect)} \tag{6}$$

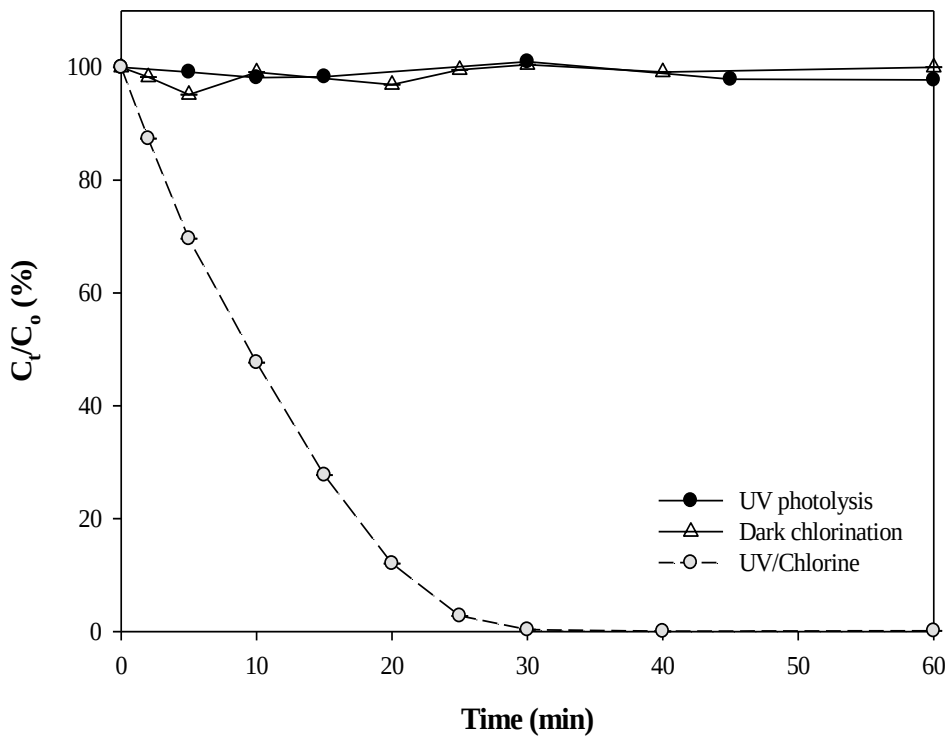

Figure 2. Degradation of cyclophosphamide (CP) using UV photolysis, dark chlorination, and UV/chlorine reactions. ($[CP]_0$ = 100 ug/L, $[Cl_2]_0$ = 6 mg/L, pH = 7, UV-B lamp = 2.2 mW/cm^2 (6 W), 312 nm, n = 2)

3.2. Degradation kinetics of cyclophosphamide during UV/ chlorination depends on chlorine dosage and pH.

It was observed in the study of 3.1 that the combination of UV and chlorination is most effective for the removal of cyclophosphamide (CP). Therefore, all subsequent processes followed the UV/chlorine process. The changes in the degradation kinetic of CP under different conditions were examined by adjusting the concentration of free chlorine and pH.

3.2.1. Degradation kinetics depends on chlorine dosage

Removal rate constants of cyclophosphamide during UV/chlorine process depends on free chlorine concentration is shown on Figure 3 and Table 7. The reactions followed pseudo-first-order kinetics. The rate constant was increased as more chlorine was injected. When the free chlorine concertation was increased from 0.4 to 6 mg/L, k_{obs} also increased significantly from 3.43×10^{-2} min^{-1} ($R^2 = 0.89$) to 1.98×10^{-1} min^{-1} ($R^2 = 0.93$). However, when the concertation of free chlorine was increased 6 to 14 mg/L, k_{obs} increased slightly to 2.35×10^{-1} min^{-1} ($R^2 = 0.90$). As the concentration of free chlorine increased, the reactions of radicals that produced by

HOCl and OCl^- were activated, therefore the removal rate was increased. However, if the free chlorine dosage is excessive, removal efficiency was decreased due to the self-radical scavenging of FAC (Eq. (7) - (10)) (Guo et al., 2017). For that reason, the rate constant did not increase linearly with chlorine concentration.

$$\cdot OH + HOCl \rightarrow \cdot ClO + H_2O \quad (k_1 = 2.0 \times 10^9\ M^{-1}s^{-1}) \tag{7}$$

$$\cdot OH + OCl^- \rightarrow \cdot ClO + OH^- \quad (k_2 = 8.8 \times 10^9\ M^{-1}s^{-1}) \tag{8}$$

$$\cdot Cl + HOCl \rightarrow H^+ + Cl^- + \cdot ClO \quad (k_3 = 3.0 \times 10^9\ M^{-1}s^{-1}) \tag{9}$$

$$\cdot Cl + OCl^- \rightarrow Cl^- + \cdot ClO \quad (k_4 = 8.2 \times 10^9\ M^{-1}s^{-1}) \tag{10}$$

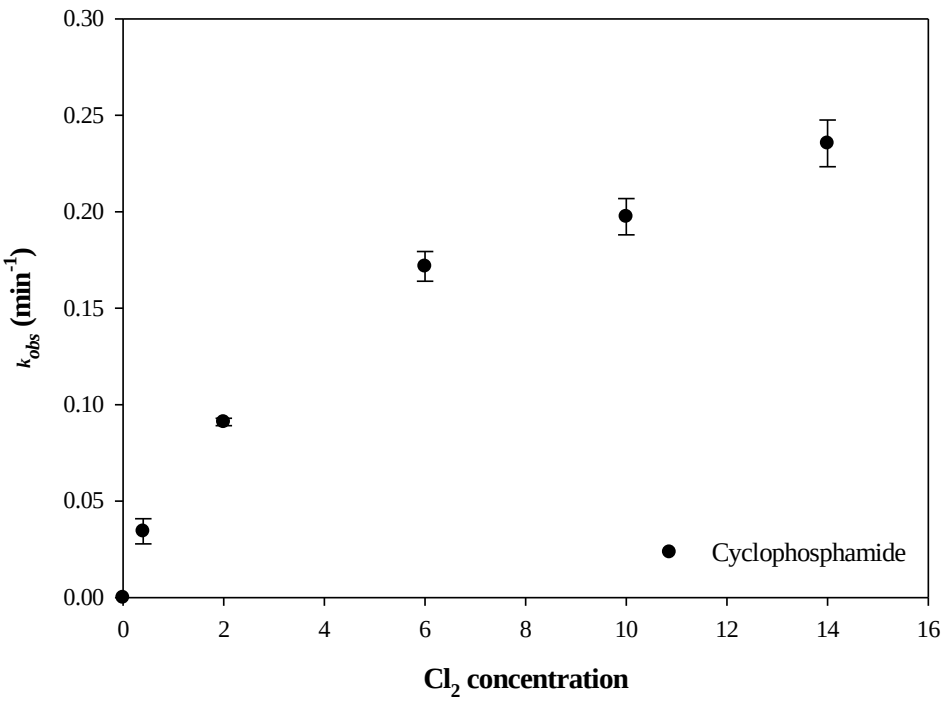

Figure 3. Removal rate constants (k_{obs}) of the cyclophosphamide (CP) by Cl_2 concentration at UV/chlorine process ($[CP]_0$ = 100 μg/L, $[Cl_2]_0$ = 0, 0.4, 2, 6, 10, 14 mg/L, pH = 7, UV lamp = 2.2 mW/cm^2 (6 W), 312 nm, n = 2).

Table 7. The pseudo-first order rate constants and coefficient of determination by various chlorine dosage.

$[Cl_2]_0$	0.4	2	6	10	14
k_{obs} (min^{-1})	0.03	0.09	0.20	0.22	0.24
R^2	0.89	0.99	0.93	0.91	0.90

3.2.2. Effect of pH

Figure 4 shows the removal rate constants of cyclophosphamide (CP) during UV/chlorine process depends on pH. The removal rate constants at pH 4 was 7.12×10^{-1} min^{-1} ($R^2 = 0.96$), pH 7 was 1.98×10^{-1} min^{-1} ($R^2 = 0.93$), and pH 10 was 0.50×10^{-1} min^{-1} ($R^2 = 0.99$). This phenomenon could explain by equation (1) – (3). At acidic condition below pH 7.6, the reaction of generating HOCl from free chlorine is dominant. Therefore, decomposition reaction of CP by OH radical and Cl radical was activated quickly.

In contrast, at basic condition over pH 7.6, the reaction of generating OCl^- from free chlorine is dominant. The OCl^- generates OH radical, but also has scavenging effect of the OH radical and reactive chlorine species (Eq. (7), (9)). Therefore, the higher ratio of OCl^- the slower removal rate of CP was observed. Also, HOCl has higher quantum yield and smaller radical scavenging effect than OCl^- (Eq. (6), (8)). For these reasons, the result of pH effect was observed that reaction rate of pH 4 (acid) > pH 7 (neutral) > pH 10 (base). The effects of pH were similar to trichloroethylene and ibuprofen (Wang, Bolton, & Hofmann, 2012; Xiang, Fang, & Shang, 2016).

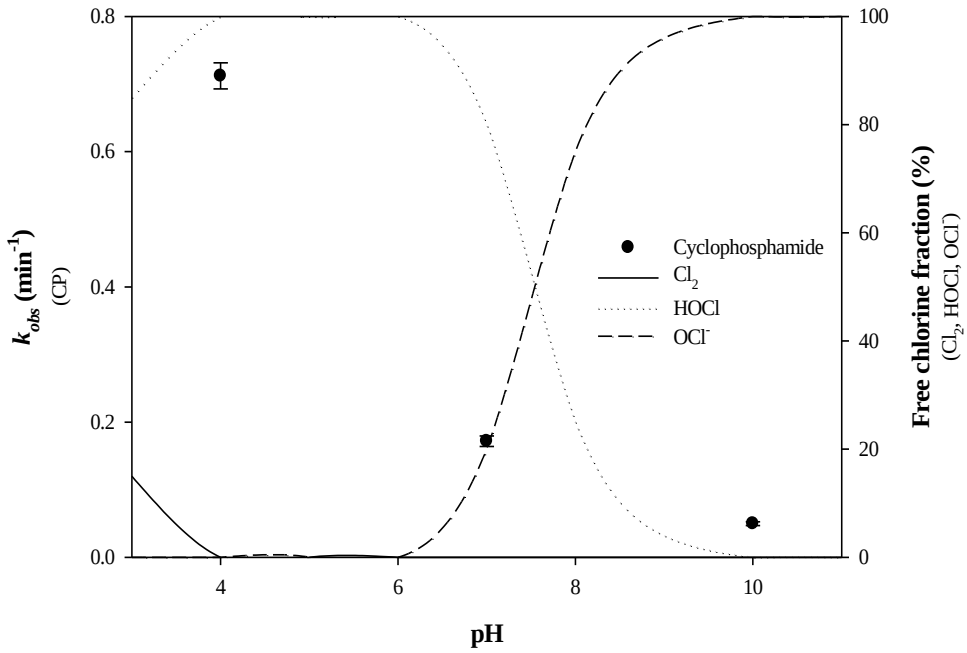

Figure 4. Removal rate constants (k_{obs}) of the cyclophosphamide (CP) by pH at UV/chlorine process ($[CP]_0$ = 100 μg/L, $[Cl_2]_0$ = 6 mg/L, pH = 4, 7, 10, UV lamp = 2.2 mW/cm^2 (6 W), 312 nm, n = 2).

Table 8. The pseudo-first order rate constants and coefficient of determination by various pH.

pH	**4**	**7**	**10**
k_{obs} **(min^{-1})**	0.71	0.20	0.05
R^2	0.96	0.93	0.99

3.3 Mineralization and identification of byproducts of cyclophosphamide during UV/chlorine process

3.3.1. Mineralization by total organic carbon (TOC)

The mineralization degree through analyzing TOC concentration during UV/chlorine process was shown in Figure 5. Due to limit of detection (LOD) of TOC analyzer, initial concentration of cyclophosphamide (CP) and the free chlorine concentration was adjusted to a removal rate constant similar to that at 100 μg / L (k_{obs} = 1.95× 10^{-1} min^{-1}, R^2 = 0.90) and to observe the stabilized time of mineralization, the reaction time was increased to 8 hours. The TOC was about 68.2 % at 40 min when CP was completely removed, and 41.6 % at two hours. It didn't show any significant change since then.

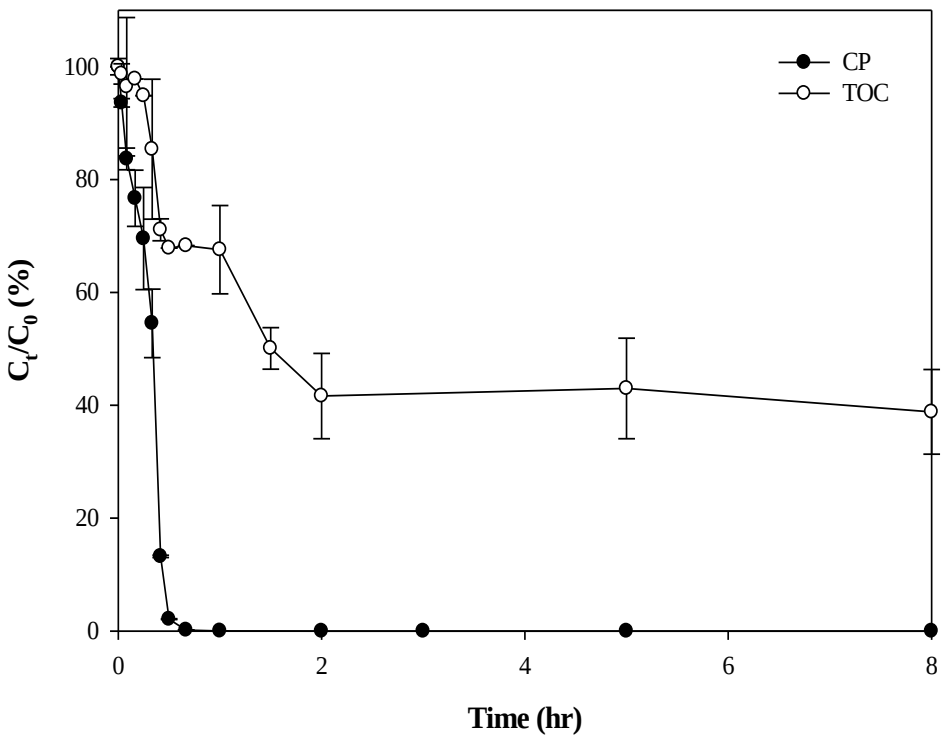

Figure 5. Degradation of cyclophosphamide (CP) and mineralization by time as measured by TOC ratio ($[CP]_0$ = 10 mg/L, $[Cl_2]_0$ = 140 mg/L, pH = 7, UV lamp = 2.2 mW/cm^2 (6 W), 312 nm, n = 2).

3.3.2. Identification of ion or inorganic byproducts

Figure 6 (a), (b) shows the time profiles of nitrate, phosphate, formate, chlorate ions, ammonia, and chlorine during UV/chlorine process using ion chromatography and Humas water analyzer. The initial concentration of cyclophosphamide (CP) and chlorine were set to 10 mg/L and 140 mg/L respectively due to LOD of instruments.

As CP was removed, ammonia and nitrate ions were produced as nitrogen byproducts. Concentration of ammonia was observed increasing trends at the beginning of the reaction but decreased over time. The maximum concentration was 0.92 mg/L at 30 min. Nitrate ion increased sharply up to 2 hours, but after that it became almost equilibrium (3.3 mg/L). The sum of the produced nitrogen byproducts accounted for 86% of the nitrogen conversion that from CP. Nitrate ion was also detected in study of removing 1-H benzotriazole by UV-A/chlorine process (365 nm) (Lee, Kim, Lee, Lee, & Zoh, 2018). In the study of Lee et al., 2018, conversion of 1-H benzotriazole-nitrogen to nitrate ion was 9% in 12 hours. However, in this study, 69% of CP-nitrogen to nitrate ion conversion was detected.

Phosphate ion was also observed as a phosphorus byproduct, and it showed steadily increasing trend and became almost equilibrium after 3 hours (1.1 mg/L). Total 20% of phosphorus in CP was also converted into phosphate ion. In addition,

the maximum 1.1% of carbon in CP was mineralized and detected in the form of formate ion (0.1 mg/L). It showed the trend of rapidly increasing at the beginning of the reaction and steadily decreasing after 90 min. Also, formate ion reacts with OH radical and form carbon dioxide (Eq. (11), (12)) (Bielski & Richter, 1977).

$$HCOO^- + HO \rightarrow COO^- + H_2O \quad (11)$$

$$COO^- + O_2 \rightarrow O_2^- + CO_2 \quad (12)$$

The concentration of chlorate ion was gradually increased and reached to almost equilibrium at 3 hours. The conversion of free chlorine to chlorate ion was maximum 1.0% at pH 7 (3.4 mg/L) in this study. It is lower than 9% that observed by Buxton and Subhani (Buxton & Subhani, 1972) when hypochlorite (OCl^-) was exposed to UV light 313 nm.

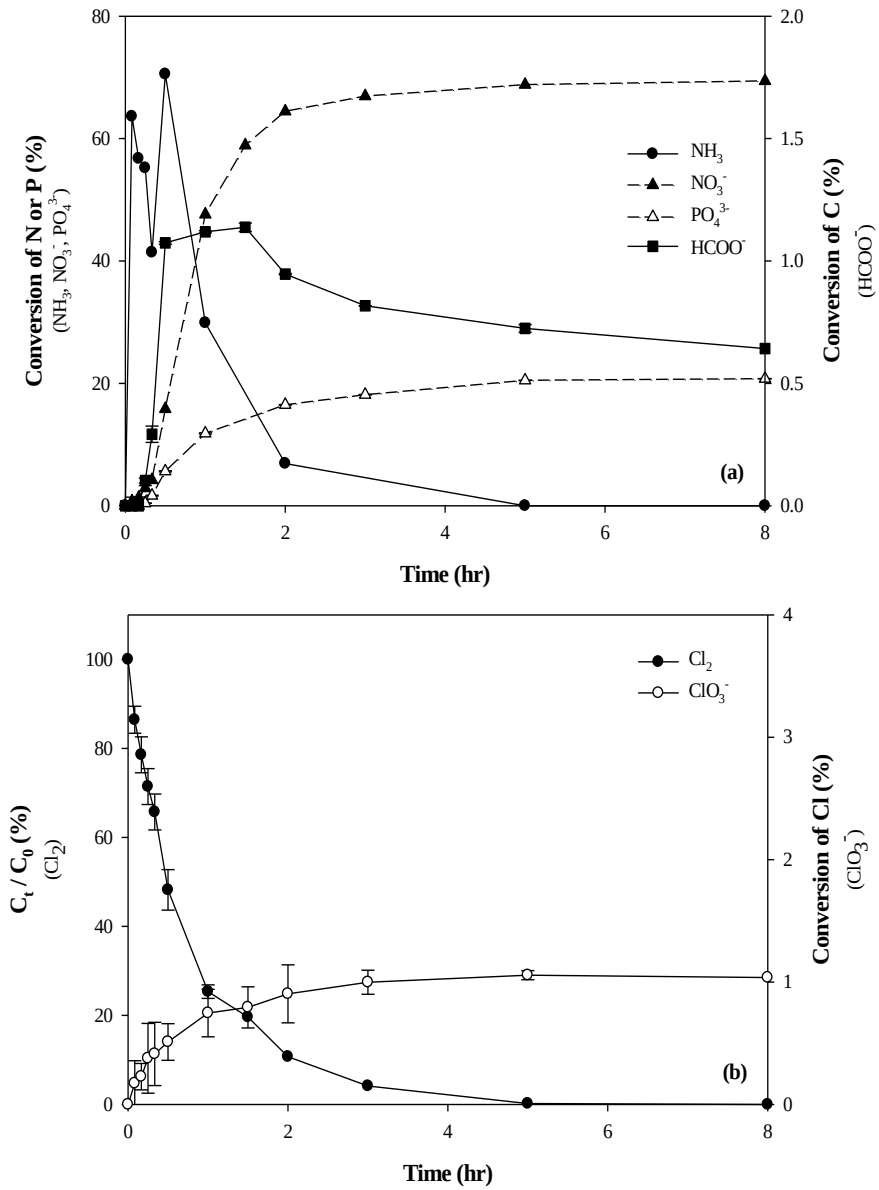

Figure 6. Time profiles of nitrate, phosphate, formate, and chlorate ions, ammonia, and chlorine during UV/chlorine process ($[CP]_0$ = 10 mg/L, $[Cl_2]_0$ = 140 mg/L, pH = 7, UV lamp = 2.2 mW/cm^2 (6 W), 312 nm, n = 2).

3.3.3. Identification of organic byproducts

Figure 7 shows the time profiles of identified organic byproducts detected by LC-qTOF-MS. The reaction time was set to 3 hours, because concentration of TOC was not changed after 2 hours and ion byproducts do not show any significant trend change after 2 hours. Total seven byproducts were identified. Among them, five were detected at positive mode of method 1 on Table 5 (byproduct 1, byproduct 3, byproduct 5, byproduct 6, byproduct 7). Two byproducts were detected in negative mode of method 1 (byproduct 4) and method 2 (byproduct 2), respectively. The detailed information of identified byproducts is on Table 10.

The peak area of byproduct 5 was the highest, following by byproduct 6 and byproduct 7. These three byproducts have highest peak area at 30 min when cyclophosphamide (CP) was 99.9% removed and decreased thereafter. Byproduct 3 showed the highest peak area at 15 min and then decreased. Byproduct 1, Byproduct 2, and Byproduct 4 showed consistently low peak area and then decreased. All identified byproducts were removed before 180 min.

Figure 8 shows that proposed pathway of identified byproducts. Byproduct 5 ($[M+H]^+ = 259.02$) is a compound which hydrogen atom is removed from 3rd and 4th positions of the ring of CP. Byproduct 6 ($[M+H]^+ = 275.01$), which called 4-ketocyclophosphamide, was produced by dropping one hydrogen atom at the 3rd

position of the ring of byproduct 5 and attaching OH radical. Byproduct 7 ($[M+Na]^+$ = 299.01) was produced by detaching one hydrogen atom at 3rd position of the ring and attaching the OH radical similar to byproduct 6. Byproduct 2 ($[M+HCOO]^-$ = 237.10) was generated hydrogen atom was attached at both ends of the P-N bond, after Cl atom was detached. Byproduct 3, so called dechloroethylcyclophosphamide was produced by cut of N-C bond of the P-N bond branch. Byproduct 4 ($[M+HCOO]^-$ = 257.01) was generated by removing two hydrogen atoms of the 3rd positions of the ring of byproduct 3 and attaching one oxygen atom. Last, byproduct 1 ($[M+H]^+$ = 142.02), which called bis(2-chloroethyl)amine, was formed detaching from ring structure of parent compound. The formation orders of the byproduct 5, 6 and byproduct 3,4 could be explained by the structure of byproducts and orders of the formation and removal which shown as peak areas at Figure 7.

Byproduct 4 was also reported by Ofiarska (Ofiarska et al., 2016) with H^+ adduct. However, in this study, it was found with $HCOO^-$ adduct. Lai (Lai et al., 2015) found byproduct 1, byproduct 3, and byproduct 6 with adduct H^+, same as this study. Byproduct 3, byproduct 5, byproduct 6, and byproduct 7 were also detected by the both UV/H_2O_2 and UV/TiO_2 processes (Lutterbeck et al., 2015). Byproduct 7 was detected with Na^+ adduct in this study, and the three except byproduct 7 were same. The sum of the peak area of identified byproducts was only for 15% compared to parent compound. It implies that unidentified byproducts are still exist in the treated wastewater.

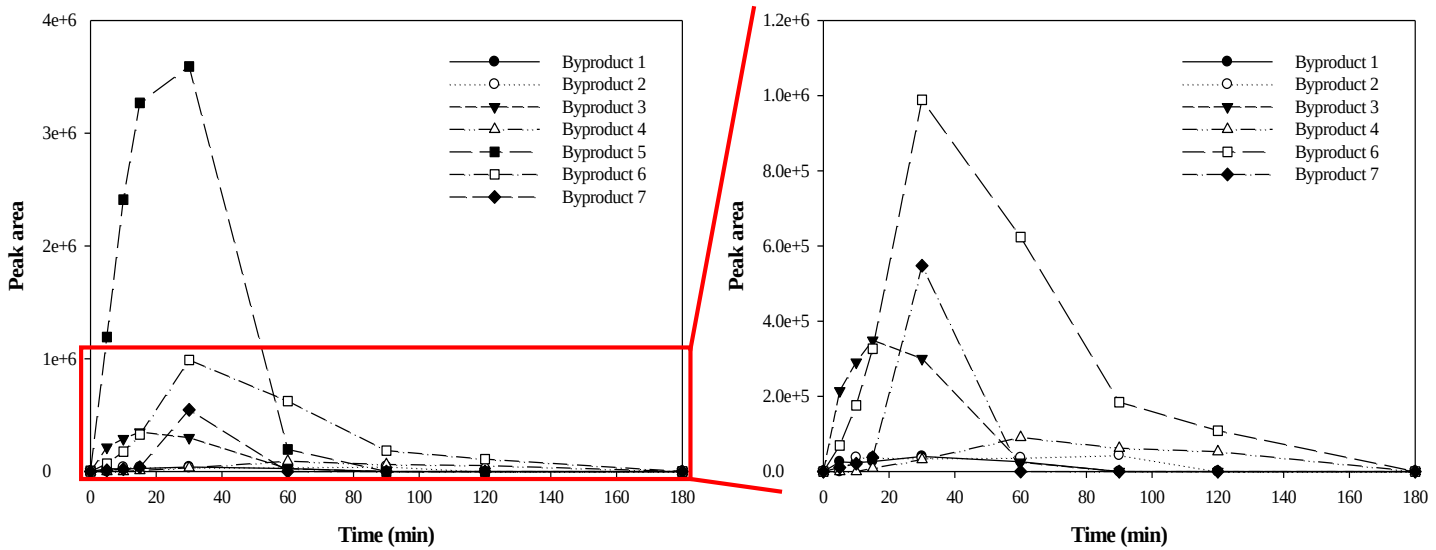

Figure 7. Time profiles of seven byproducts of cyclophosphamide (CP) during UV/chlorine process ($[CP]_0$ = 1.0 mg/L, $[Cl_2]_0$ = 10 mg/L, pH = 7, UV lamp = 2.2 mW/cm^2 (6 W), 312 nm, n = 2).

Table 9. Result of mass fragment analysis about identified byproducts.

Component	Formula	Observed m/z (Adducts)	Mass error (Da)	Mass error (ppm)	Observed RT (min)	Fragments m/z (mass error)	Structure
Byproduct 1	$C_4H_9Cl_2N$	142.0186 (+ H)	0.1	0.8	3.57	107.0478 (-1.8 mDa)	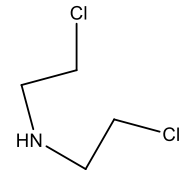
Byproduct 2	$C_7H_{17}N_2O_2P$	237.1014 (+ HCOO)	0.5	1.9	8.84	-	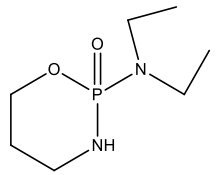
Byproduct 3	$C_5H_{12}ClN_2O_2P$	199.0398 (+ H)	0.0	0.0	4.37	78.0107 (0.2 mDa) 120.0208 (-0.1 mDa) 149.0600 (-0.1 mDa) 159.0088 (0.4 mDa) 171.0081 (-0.4 mDa) 173.0248 (0.7 mDa)	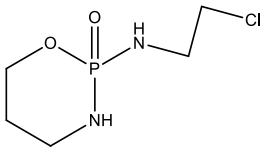

Byproduct 4	$C_5H_{12}ClN_2O_3P$	257.0092 (+ HCOO)	-0.8	-3.0	4.14	197.0268 (1.7 mDa)	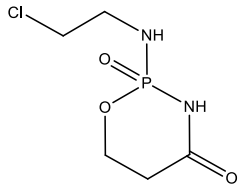
Byproduct 5	$C_7H_{15}Cl_2N_2O_2P$	259.0170 (+ H)	0.5	2.0	5.88	106.0417 (-0.1 mDa) 114.0103 (0.0 mDa) 120.0210 (0.1 mDa) 140.0029 (0.1 mDa) 167.9978 (0.3 mDa) 189.0785 (-0.2 mDa) 197.0241 (-0.1 mDa) 223.0405 (0.7 mDa) 225.0548 (-0.6 mDa)	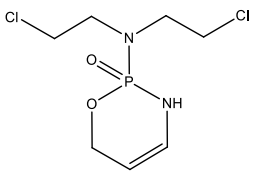
Byproduct 6	$C_7H_{16}Cl_2N_2O_3P$	275.0114 (+ H)	0.1	0.2	4.97	114.0108 (0.5mDa) 167.9979 (0.3mDa) 185.9633 (-0.4 mDa) 239.0341 (-0.6 mDa) 241.0048 (-1.1 mDa)	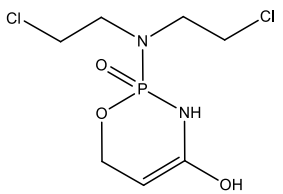

Byproduct 7	$C_7H_{16}Cl_2N_2O_3P$	299.0083 (+ Na)	-0.7	-2.3	4.84	56.0494 (-0.1 mDa) 114.0098 (-0.5 mDa) 142.0180 (-0.5 mDa) 203.9734 (-0.8 mDa) 221.0010 (0.2 mDa) 259.0156 (-0.9 mDa)	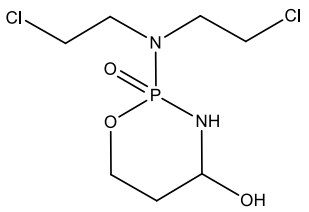

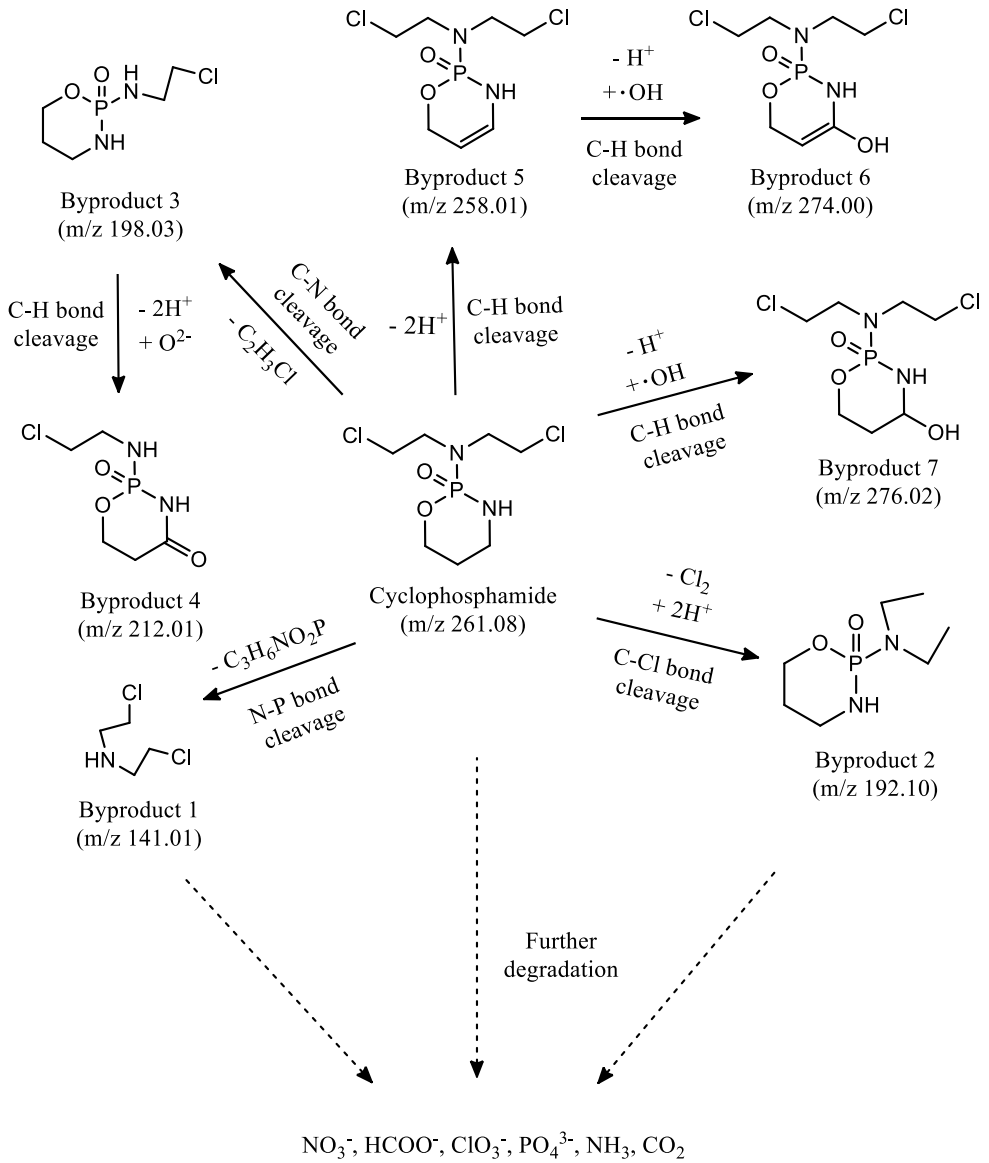

Figure 8. Predicted degradation pathway of Cyclophosphamide during UV / chlorine process.

3.4. Acute Toxicity Test

The result of the acute toxicity test called microtox was shown in Figure 9 (a). Microtox test was conducted using bioluminescent bacterium *Vibrio fisheri*. The *V. fisheri* were exposed to untreated and treated samples for 15 min, then measured luminescence and the inhibition of luminescence was expressed as the ration of the untreated sample. The luminescence was steadily decreased until 15 min, and significantly decreased from 15 to 60 min. After 60 min, the luminescence was gradually diminished again and reached to equilibrium after 120 min.

Figure 9 (b) shows the estimated toxicity of each identified byproducts run by QSAR software (OECD Tool Box V.4.2), and LC 50 values were estimated about *Pimephales promelas*. The toxicity prediction was run for cyclophosphamide (CP), byproduct 1, byproduct 2, byproduct 5, and byproduct 7. For byproduct 4, byproduct 3, and byproduct 6 were unable to estimate the toxicity since structure prediction was impossible. Result of running QSAR, the LC 50 value of the byproducts were less than that of CP, the parent compound.

The time profile of byproduct identified and toxicity in this study were not matched. The UV/chlorine process cannot completely mineralize the CP, it may due to some of the unidentified byproducts which have high toxicity. Also, the toxicity of each identified byproduct and the toxicity of the actual mixture may be different,

so that the result of QSAR toxicity test were not matched to toxicity that measured by *V. fisheri*. There is a study (Russo et al., 2018) that mortality increased when *B. calyciflorus* and *C. dubia* were exposed to CP samples that irradiated UV lamp. Therefore, further research on byproducts and toxicity is needed to accurately predict the toxicity.

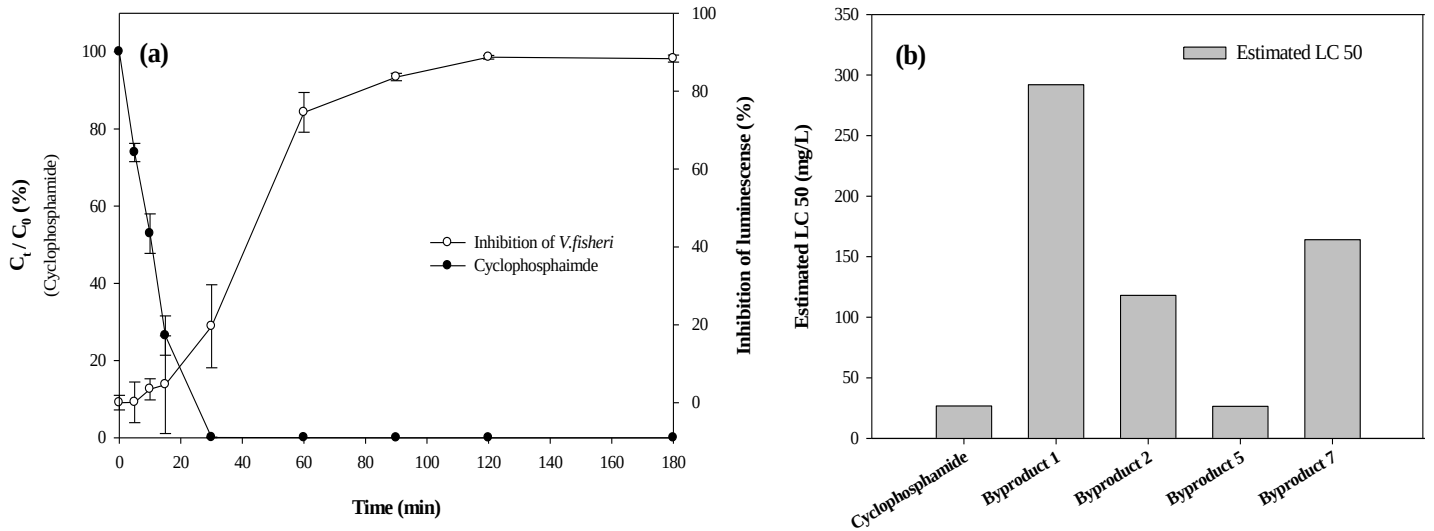

Figure 9. (a) Removal of cyclophosphamide (CP), and acute toxicity by luminescence inhibition of *V. fisheri*, **(b)** Estimated toxicity of each byproduct using QSAR Tool box. ($[CP]_0$ = 1.0 mg/L, $[Cl_2]_0$ = 10 mg/L, pH = 7, UV lamp = 2.2 mW/cm^2 (6 W), 312 nm, n = 2).

4. Conclusions

In this study, UV photolysis, dark chlorination, and UV/chlorine process were compared and it was found that only the UV/chlorine process could completely remove cyclophosphamide (CP) in 40 min. This is due to the synergistic effect of the UV lamp and free chlorine, and production radicals were increased. It was also found that the removal of CP was accelerated by increasing the concentration of free chlorine and lowering the pH.

In UV/chlorine process, 56.3% of the CP was mineralized for 8 hours and organic, inorganic and ion byproducts were formed during the process. Total seven organic byproducts (m/z = 141.01, 192.10, 198.03, 212.01, 258.01, 274.00, 276.02) were identified while five inorganic byproducts (NH_3, NO_3^-, $HCOO^-$, PO_4^{3-}, ClO_3^-) were identified in this study. During the toxicity test using *V. fisheri*, it was observed that the luminescence was lowered as the UV/chlorine process proceeded.

This study was conducted to investigate the removal kinetics, byproducts and toxicity of CP, which is one of the anticancer drugs detected by high concentration and not well treated in hospital wastewater, through the UV-B/ chlorine process. This study can be used as a reference material for establishment of treatment system in hospital wastewater treatment plant.

5. Reference

Bielski, B. H., & Richter, H. W. (1977). A study of the superoxide radical chemistry by stopped-flow radiolysis and radiation induced oxygen consumption. *Journal of the American Chemical Society, 99*(9), 3019-3023.

Buerge, I. J., Buser, H.-R., Poiger, T., & Müller, M. D. (2006). Occurrence and fate of the cytostatic drugs cyclophosphamide and ifosfamide in wastewater and surface waters. *Environmental science & technology, 40*(23), 7242-7250.

Busetti, F., Linge, K. L., & Heitz, A. J. J. o. C. A. (2009). Analysis of pharmaceuticals in indirect potable reuse systems using solid-phase extraction and liquid chromatography–tandem mass spectrometry. *1216*(31), 5807-5818.

Buxton, G., & Subhani, M. (1972). Radiation chemistry and photochemistry of oxychlorine ions. Part 2.—Photodecomposition of aqueous solutions of hypochlorite ions. *Journal of the Chemical Society, Faraday Transactions 1: Physical Chemistry in Condensed Phases, 68*, 958-969.

Catastini, C., Mullot, J.-U., Boukari, S., Mazellier, P., Levi, Y., Cervantes, P., & Ormsby, J.-N. J. E. J. o. W. Q. (2008). Assessment of antineoplastic drugs in effluents of two hospitals. *39*, 171-180.

Česen, M., Kosjek, T., Laimou-Geraniou, M., Kompare, B., Širok, B., Lambropolou, D., & Heath, E. (2015). Occurrence of cyclophosphamide and ifosfamide in aqueous environment and their removal by biological and abiotic wastewater treatment processes. *Science of the Total Environment, 527*, 465-473.

Constantin, L. A., Cristea, I., Nitoi, I., Constantin, A. M., & Nechifor, G. (2017). Kinetics of Cyclophosphamide and Ifosfamide Degradation from Aqueous System via TiO2 Assisted Photocatalysis.

Fang, J., Fu, Y., & Shang, C. (2014). The roles of reactive species in micropollutant degradation in the UV/free chlorine system. *Environmental science &*

technology, 48(3), 1859-1868.

Fernández, L., Hernández, C., Bataller, M., Veliz, E., Lopez, A., Ledea, O., & Padron, S. (2010). Cyclophosphamide degradation by advanced oxidation processes. *Water and Environment Journal, 24*(3), 174-180.

Franquet-Griell, H., Medina, A., Sans, C., & Lacorte, S. (2017). Biological and photochemical degradation of cytostatic drugs under laboratory conditions. *Journal of hazardous materials, 323*, 319-328.

Garcia-Ac, A., Broséus, R., Vincent, S., Barbeau, B., Prévost, M., & Sauvé, S. (2010). Oxidation kinetics of cyclophosphamide and methotrexate by ozone in drinking water. *Chemosphere, 79*(11), 1056-1063.

Glaze, W. H., Kang, J.-W., & Chapin, D. H. (1987). The chemistry of water treatment processes involving ozone, hydrogen peroxide and ultraviolet radiation.

Glaze, W. H., & Kang, J. W. (1989). Advanced oxidation processes. Description of a kinetic model for the oxidation of hazardous materials in aqueous media with ozone and hydrogen peroxide in a semibatch reactor. *Industrial & engineering chemistry research, 28*(11), 1573-1580.

Gómez-Canela, C., Cortés-Francisco, N., Oliva, X., Pujol, C., Ventura, F., Lacorte, S., & Caixach, J. (2012). Occurrence of cyclophosphamide and epirubicin in wastewaters by direct injection analysis–liquid chromatography–high-resolution mass spectrometry. *Environmental Science and Pollution Research, 19*(8), 3210-3218.

Guo, K., Wu, Z., Shang, C., Yao, B., Hou, S., Yang, X., . . . Fang, J. (2017). Radical chemistry and structural relationships of PPCP degradation by UV/chlorine treatment in simulated drinking water. *Environmental science & technology, 51*(18), 10431-10439.

IARC. (2016). List of classifications, volumes 1-115.

Isidori, M., Lavorgna, M., Russo, C., Kundi, M., Žegura, B., Novak, M., . . . de Alda, M. L. J. E. p. (2016). Chemical and toxicological characterisation of anticancer drugs in hospital and municipal wastewaters from Slovenia

and Spain. *219*, 275-287.

Jalali, A. S., Hasanzadeh, S., & Malekinejad, H. J. C. J. o. N. M. (2012). Achillea millefolium inflorescence aqueous extract ameliorates cyclophosphamide-induced toxicity in rat testis: stereological evidences. *10*(4), 247-254.

Lai, W. W.-P., Chuang, Y.-C., & Lin, A. Y.-C. (2017). The effects and the toxicity increases caused by bicarbonate, chloride, and other water components during the UV/TiO2 degradation of oxazaphosphorine drugs. *Environmental Science and Pollution Research, 24*(17), 14595-14604.

Lai, W. W.-P., Lin, H. H.-H., & Lin, A. Y.-C. (2015). TiO 2 photocatalytic degradation and transformation of oxazaphosphorine drugs in an aqueous environment. *Journal of hazardous materials, 287*, 133-141.

Lee, J.-E., Kim, M.-K., Lee, J.-Y., Lee, Y.-M., & Zoh, K.-D. (2018). Degradation Kinetics and Pathway of 1H-benzotriazole during UV/chlorination Process. *Chemical Engineering Journal*.

Luo, Y., Guo, W., Ngo, H. H., Nghiem, L. D., Hai, F. I., Zhang, J., . . . Wang, X. C. J. S. o. t. t. e. (2014). A review on the occurrence of micropollutants in the aquatic environment and their fate and removal during wastewater treatment. *473*, 619-641.

Lutterbeck, C. A., Machado, Ê. L., & Kümmerer, K. (2015). Photodegradation of the antineoplastic cyclophosphamide: a comparative study of the efficiencies of UV/H 2 O 2, UV/Fe 2+/H 2 O 2 and UV/TiO 2 processes. *Chemosphere, 120*, 538-546.

Margot, J., Rossi, L., Barry, D. A., & Holliger, C. J. W. I. R. W. (2015). A review of the fate of micropollutants in wastewater treatment plants. *2*(5), 457-487.

Moldovan, Z. (2006). Occurrences of pharmaceutical and personal care products as micropollutants in rivers from Romania. *Chemosphere, 64*(11), 1808-1817.

Negreira, N., de Alda, M. L., & Barceló, D. J. S. o. t. T. E. (2014). Cytostatic drugs

and metabolites in municipal and hospital wastewaters in Spain: filtration, occurrence, and environmental risk. *497*, 68-77.

Ofiarska, A., Pieczyńska, A., Borzyszkowska, A. F., Stepnowski, P., & Siedlecka, E. M. (2016). Pt–TiO 2-assisted photocatalytic degradation of the cytostatic drugs ifosfamide and cyclophosphamide under artificial sunlight. *Chemical Engineering Journal, 285*, 417-427.

Russo, C., Lavorgna, M., česen, M., Kosjek, T., Heath, E., & Isidori, M. (2018). Evaluation of acute and chronic ecotoxicity of cyclophosphamide, ifosfamide, their metabolites/transformation products and UV treated samples. *Environmental Pollution, 233*, 356-363.

Schwarzenbach, R. P., Egli, T., Hofstetter, T. B., Von Gunten, U., Wehrli, B. J. A. R. o. E., & Resources. (2010). Global water pollution and human health. *35*, 109-136.

Steger-Hartmann, T., Kümmerer, K., & Hartmann, A. (1997). Biological degradation of cyclophosphamide and its occurrence in sewage water. *Ecotoxicology and environmental safety, 36*(2), 174-179.

Steger-Hartmann, T., Kümmerer, K., & Schecker, J. (1996). Trace analysis of the antineoplastics ifosfamide and cyclophosphamide in sewage water by twostep solid-phase extraction and gas chromatography-mass spectrometry. *Journal of Chromatography A, 726*(1-2), 179-184.

Ternes, T. A., Bonerz, M., Herrmann, N., Löffler, D., Keller, E., Lacida, B. B., & Alder, A. C. (2005). Determination of pharmaceuticals, iodinated contrast media and musk fragrances in sludge by LC tandem MS and GC/MS. *Journal of Chromatography A, 1067*(1-2), 213-223.

Wang, D., Bolton, J. R., & Hofmann, R. (2012). Medium pressure UV combined with chlorine advanced oxidation for trichloroethylene destruction in a model water. *Water research, 46*(15), 4677-4686.

Xiang, Y., Fang, J., & Shang, C. (2016). Kinetics and pathways of ibuprofen degradation by the UV/chlorine advanced oxidation process. *Water research, 90*, 301-308.

Yin, J., Shao, B., Zhang, J., & Li, K. (2010). A preliminary study on the occurrence of cytostatic drugs in hospital effluents in Beijing, China. *Bulletin of environmental contamination and toxicology, 84*(1), 39.

Zhang, Y., Xiao, Y., Zhang, J., Chang, V. W., & Lim, T.-T. (2017). Degradation of cyclophosphamide and 5-fluorouracil in water using UV and UV/H 2 O 2: Kinetics investigation, pathways and energetic analysis. *Journal of Environmental Chemical Engineering, 5*(1), 1133-1139.

Supplementary materials

Figure S1. Molar absorption coefficient at UV wavelength according to pH of cyclophosphamide.

Figure S2. Total ion chromatogram (TIC) and extracted ion chromatogram (XIC) of Byproduct 1.

Figure S3. TIC and XIC of Byproduct 2.

Figure S4. TIC and XIC of Byproduct 3.

Figure S5. TIC and XIC of Byproduct 4.

Figure S6. TIC and XIC of Byproduct 5.

Figure S7. TIC and XIC of Byproduct 6.

Figure S8. TIC and XIC of Byproduct 7.

Text S1. Explanation of Figure S9 and S10.

Figure S9. Degradation of cyclophosphamide (CP) using UV-C lamp and mineralization as measured by TOC concentration.

Figure S10. Time profiles of nitrate, phosphate, formate, and chlorate ions, ammonia, and chlorine during UV-C/chlorine process.

Text S2. Explanation of Figure S11.

Figure S 11. TOC ratio and luminescence inhibition of *V. fisheri* when additional chlorine was injected at 2 hr ($[CP]_0$ = 10 mg/L, $[Cl_2]_0$ = 140 mg/L, pH = 7, UV lamp = 2.0 mW/cm^2 (6 W), 245 nm, n = 2).

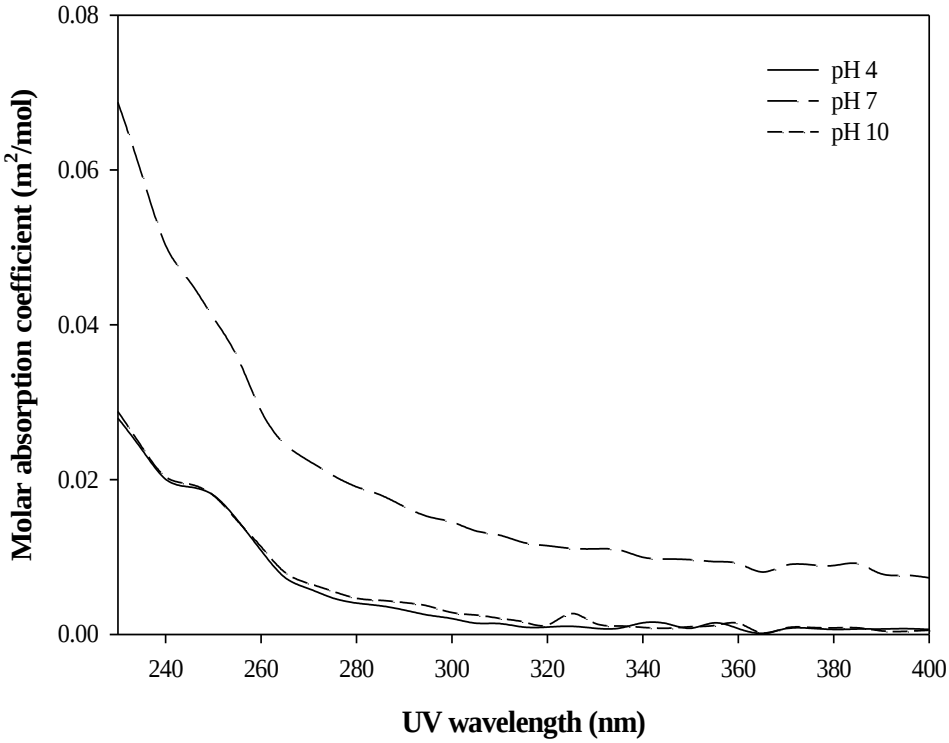

Figure S1. Molar absorption coefficient at UV wavelength according to pH of cyclophosphamide ($[CP]_0$ = 0.1 mg/L, pH = 4, 7, 10).

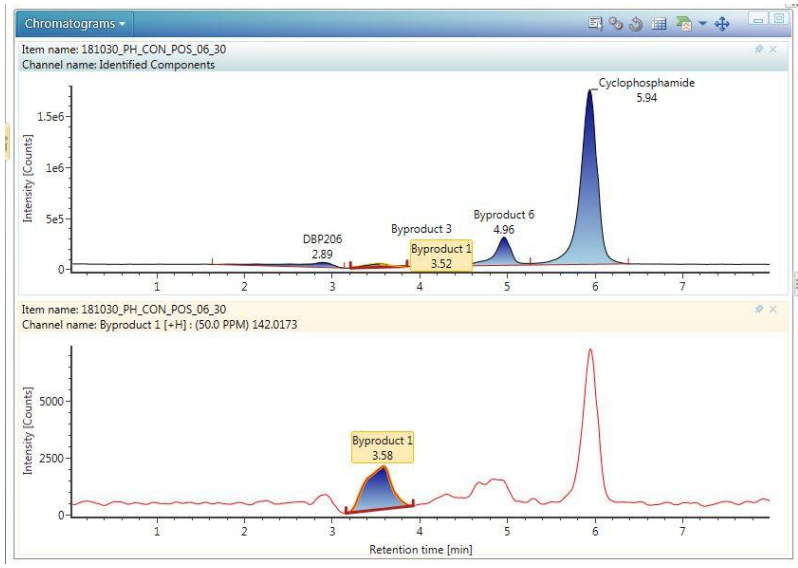

Figure S2. Total ion chromatogram (TIC) and extracted ion chromatogram (XIC) of Byproduct 1.

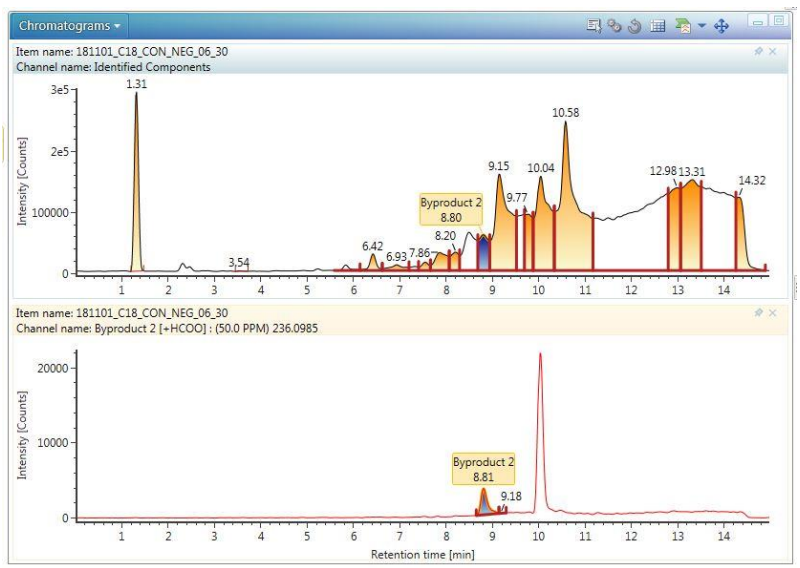

Figure S3. TIC and XIC of Byproduct 2.

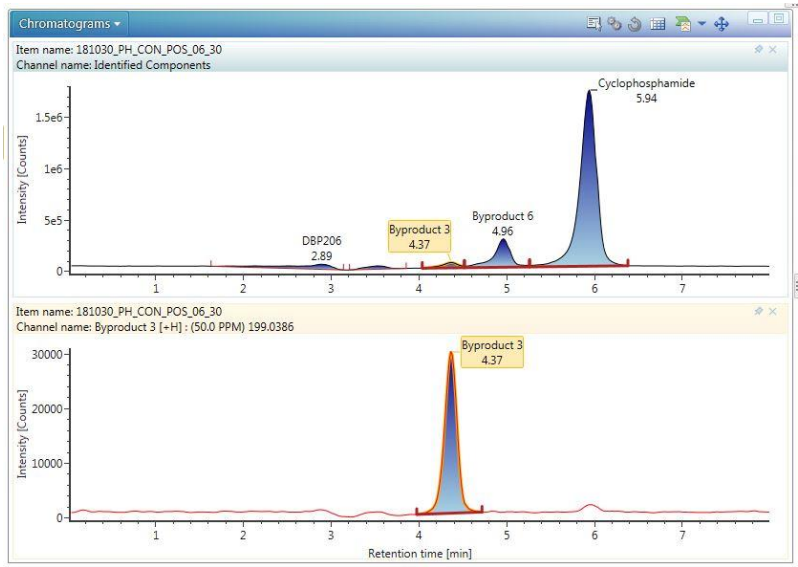

Figure S4. TIC and XIC of Byproduct 3.

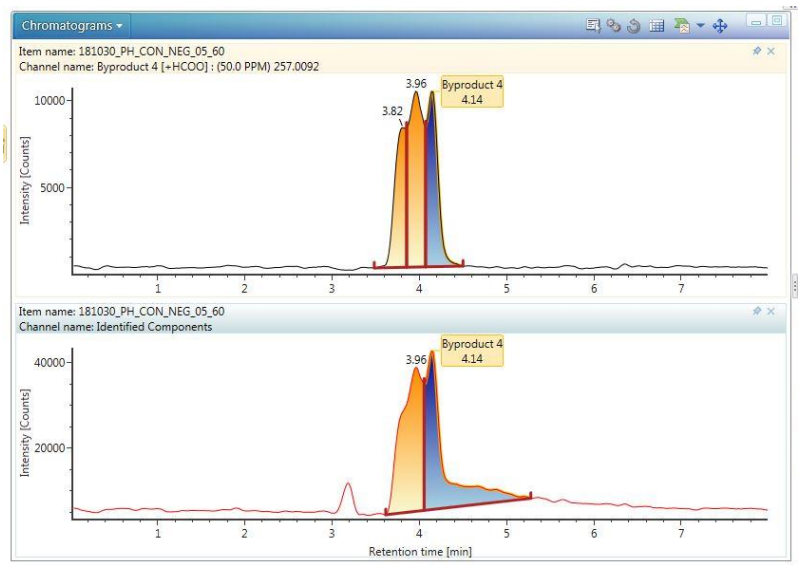

Figure S5. TIC and XIC of Byproduct 4.

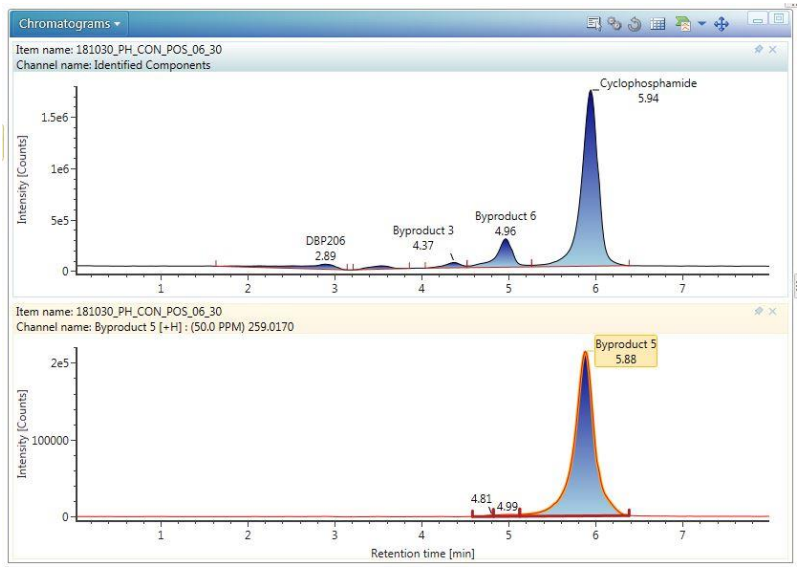

Figure S6. TIC and XIC of Byproduct 5.

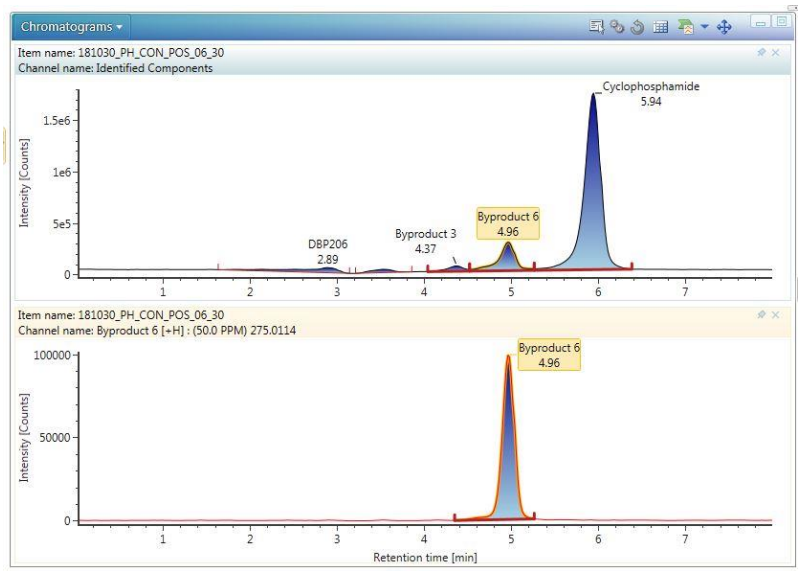

Figure S7. TIC and XIC of Byproduct 6.

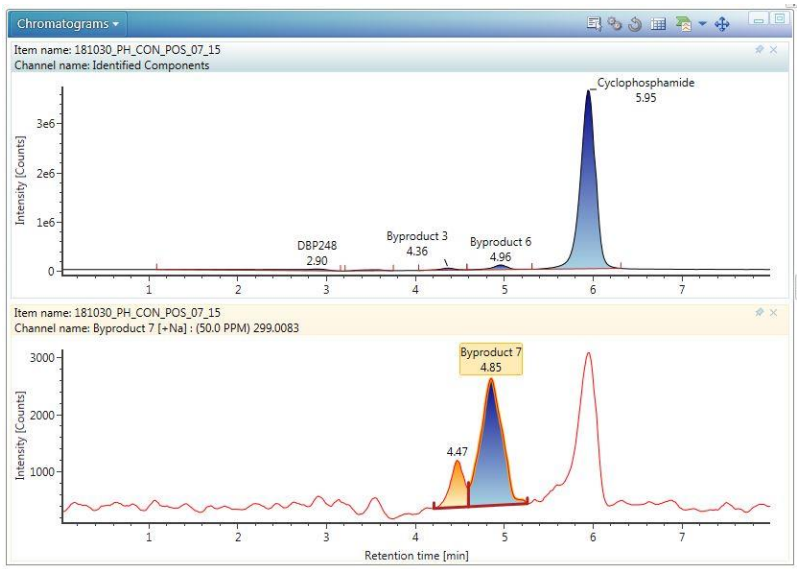

Figure S8. TIC and XIC of Byproduct 7.

Text S1. Explanation of Figure S9 and S10.

Figure S9 shows the result of removing cyclophosphamide (CP) by UV/chlorine process with UV-C lamp (245 nm) which is more destructive than UV-B lamp (312 nm). Inorganic and ionic byproducts that identified in the UV-C/chlorine process were shown at Figure S10. When the UV-C lamp was irradiated, removal rate constant (k_{obs} = 2.98 × 10^{-1} min^{-1} (R^2 = 0.92)) was higher than that of UV-B lamp. Mineralization was also observed by TOC analyzer. The TOC remained 37.8 % at 8 hr, as similar as UV-B lamp (38.8 %). However, the TOC which irradiated by UV-C lamp was deceased faster than that of UV-B lamp. In Figure S10, ammonia and formate shows higher conversion ratio than that of UV-B lamp. The conversion ratio of nitrate, phosphate and chlorate at 8hr showed similar but reached to equilibrium faster than the conversion ratio of UV-B lamp.

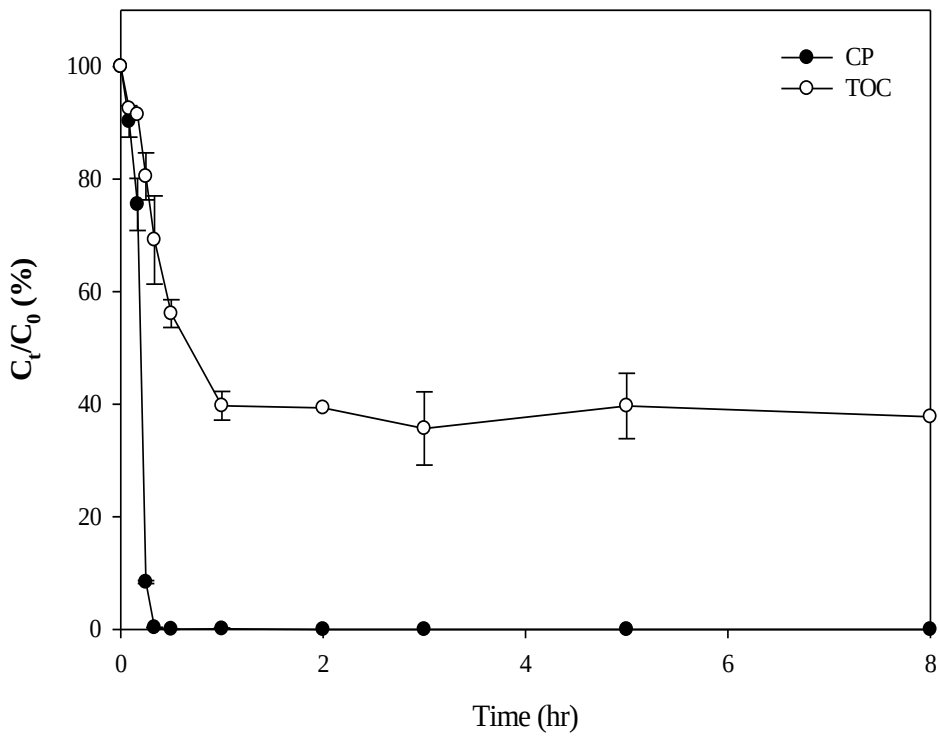

Figure S9. Degradation of cyclophosphamide (CP) using UV-C lamp and mineralization as measured by TOC ratio ($[CP]_0$ = 10 mg/L, $[Cl_2]_0$ = 140 mg/L, pH = 7, UV lamp = 2.0 mW/cm^2 (6 W), 245 nm, n = 2).

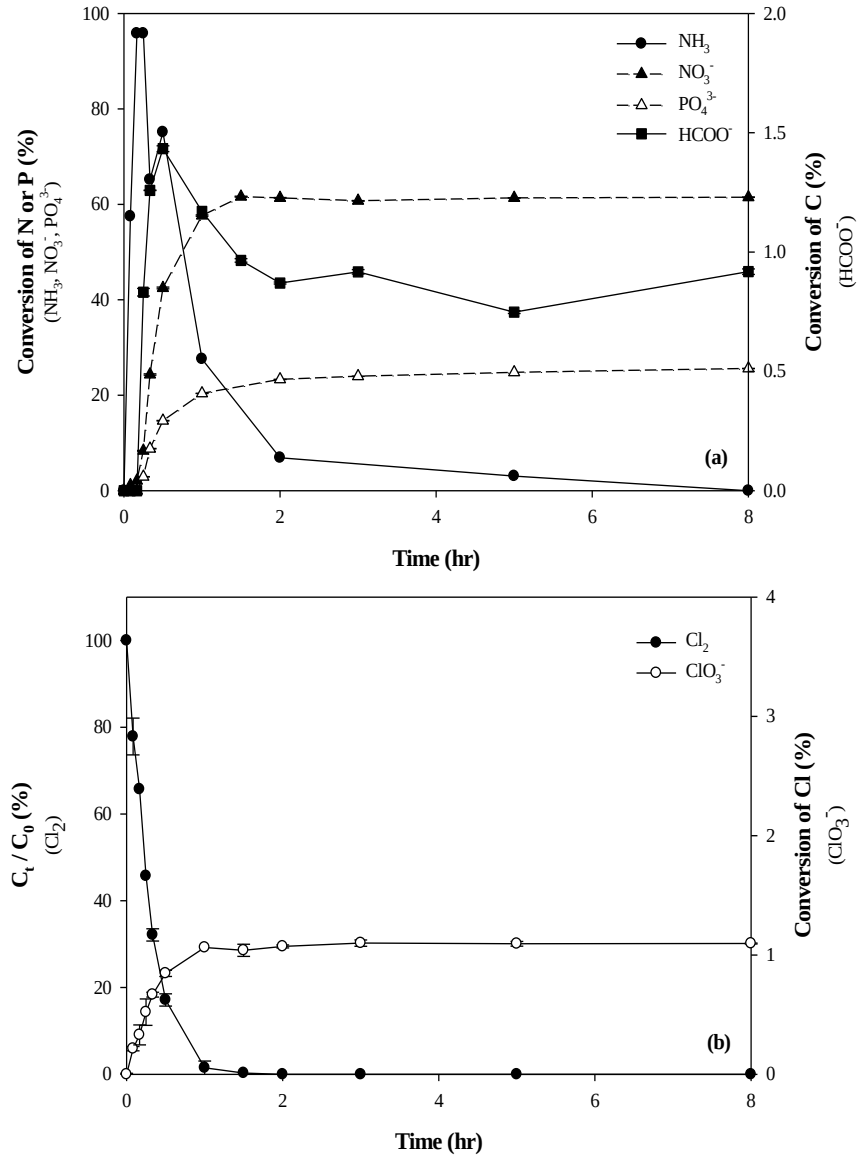

Figure S10. Time profiles of nitrate, phosphate, formate, and chlorate ions, ammonia, and chlorine during UV-C/chlorine process. ($[CP]_0$ = 10 mg/L, $[Cl_2]_0$ = 140 mg/L, pH = 7, UV lamp = 2.0 mW/cm^2 (6 W), 254 nm, n = 2).

Text S2. Explanation of Figure S11.

In Figure 9 (a) of the main text, the reason of the toxicity increased was predicted to be due to toxicity of unidentified byproducts. Therefore, to break the unidentified byproducts, chlorine was injected additionally to original concentration at just after 2 hr when TOC ratio was reached to equilibrium. Figure S11 shows the TOC and toxicity change through the additional chlorine. The TOC ratio was 18.3% at 8 hr, which was 20.5% lower than when chlorine was not added. However, the luminescence inhibition of *V. fisheri* was decreased by 22% after 2 hr, and then gradually increased. Luminescence inhibition ratio at 8 hr was similar to 2 hr that before adding additional chlorine. This phenomenon could be estimated that some of the unidentified byproducts were broken due to additional injection of chlorine, and produced new toxic byproducts which increases toxicity again. To confirm the exact result, further research is needed.

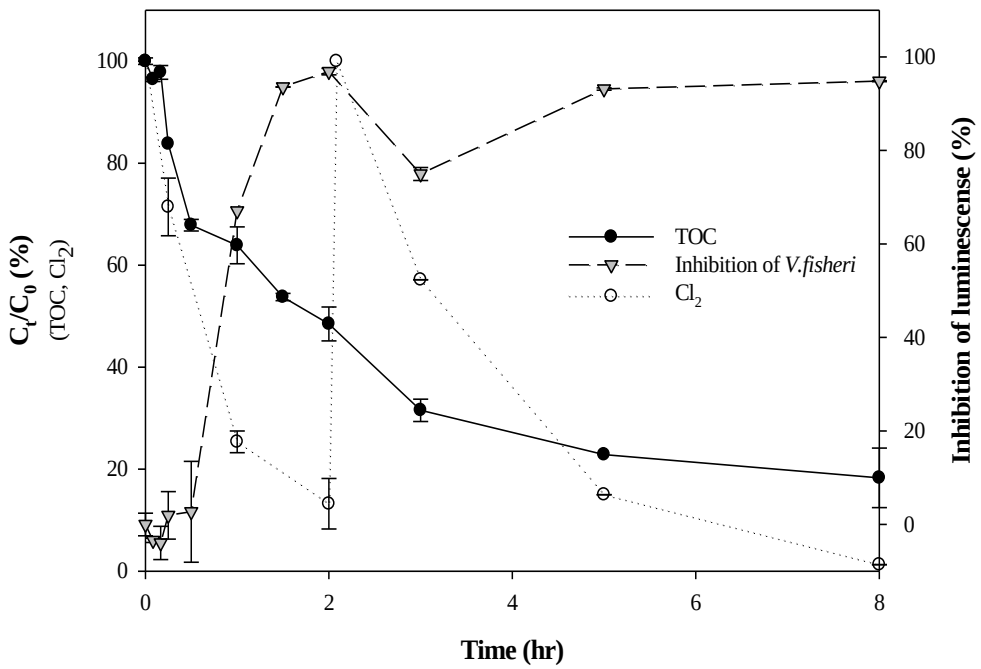

Figure S21. TOC ratio and luminescence inhibition of *V. fisheri* when additional chlorine was injected at 2 hr ($[CP]_0$ = 10 mg/L, $[Cl_2]_0$ = 140 mg/L, pH = 7, UV lamp = 2.0 mW/cm^2 (6 W), 245 nm, n = 2).

국문 초록

UV/chlorine 공정 중 Cyclophosphamide의 분해 특성과 메커니즘에 관한 연구

이 지 영

서울대학교 보건대학원

환경보건학과 환경보건학 전공

지도교수 조 경 덕

항암제 중 널리 쓰이는 cyclophosphamide는 비표적으로 장기에 손상을 주는 등 부작용이 있다. 모니터링 연구에 의하면, cyclophosphamide는 병원 폐수와 지표수 에서 검출되었다. 게다가,

Cyclophosphamide는 생분해되지 않고 일반적인 처리방법으로는 폐수 처리장에서 제거가 잘 되지 않는다. 따라서 본 연구에서는 UV-B/chlorine 공정을 이용한 cyclophosphamide 의 제거 메커니즘을 살펴보았다. Cyclophosphamide는 UV 광분해와 염소처리 방법을 통해서는 제거가 되지 않았고, UV/chlorine 공정을 통해서만 제거되었다 (k_{obs} = $1.98 \times 10\text{- min}^{-1}$ ($R^2 = 0.93$)). 이를 통하여 UV/chlorine 공정이 다른 두 공정보다 cyclophosphamide를 처리하는데 효율적이라는 것을 알 수 있다. 주입 염소 농도와 pH 변화 실험에서 염소 농도가 높을수록, pH가 산성일수록 반응 속도가 빨라졌다. 반응을 통해 8시간 동안 56.3%의 cyclophosphamide가 무기화 되었으며, 일곱가지의 유기부산물 (m/z = 141.01, 192.10, 198.03, 212.01, 258.01, 274.00, 276.02)이 LC-qTOF-MS를 통하여, 다섯 가지의 이온 또는 무기부산물 (NH_3, NO_3^-, $HCOO^-$, PO_4^{3-}, ClO_3^-)이 이온 크로마토그래피를 통하여 검출되었다. *V. fisheri*를 이용한 급성 독성실험에서 *V. fisheri*의 발광도가 최대 88% 감소하였다. 이 연구를 통하여 병원 폐수 내에 고농도로 존재하고 기존처리법으로 잘 제거되지 않는 cyclophosphamide를 UV/chlorine 공법을 통하여 제거하였다. 이 연구는 최적화를 거치면 병원 폐수처리장의 cyclophosphamide 처리법 개발 시 참고자료로 사용될 수 있을 것이다.

주요어: 시클로포스파마이드, 항암제, UV-B/chlorine 공정, 반응 부산물, 급성 독성

학번: 2017-24362